UNIDIRECTIONAL CALCIUM AND NUCLEOTIDE FLUXES IN CARDIAC SARCOPLASMIC RETICULUM

II. Experimental Results

JOSEPH J. FEHER AND F. NORMAN BRIGGS
Department of Physiology and Biophysics, Medical College of Virginia, Richmond, Virginia 23298

ABSTRACT Unidirectional calcium influx and efflux were evaluated in cardiac sarcoplasmic reticulum (SR) by ^{45}Ca–^{40}Ca exchange at steady state calcium uptake in the absence of calcium precipitating anions. Calcium efflux was partitioned into a pump-mediated efflux and a parallel passive efflux by separately measuring passive efflux referable to the steady state. Unidirectional and net ATP-ADP fluxes were measured using [^{3}H]-ATP → ADP and [^{3}H]-ADP → ATP exchanges. Methods are presented that take into account changing specific activities and sizes of the nucleotide pools during the measurement of nucleotide fluxes. The contribution of competent and incompetent vesicles to the unidirectional and net nucleotide fluxes was evaluated from the specific activity of these fluxes in incompetent vesicles and from the fraction of vesicles that were incompetent. The results indicate that, in cardiac SR, unidirectional calcium fluxes are larger than the unidirectional nucleotide fluxes contributed by competent vesicles. Because the net ATPase rate of competent vesicles is similar to the parallel passive efflux, it appears that cardiac SR Ca-ATPase tightly couples ATP hydrolysis to calcium transport even at static head, with a coupling ratio near 1.0.

INTRODUCTION

It has been known for some time that steady state calcium uptake by sarcoplasmic reticulum (SR) is accompanied by a rapid calcium-calcium exchange (Martonosi and Feretos, 1964) and rapid ATP-ADP exchange (Ebashi and Lipmann, 1962). The relation between these exchanges, however, has only recently been investigated. Makinose (1973) first simultaneously measured ATP-ADP exchange and calcium fluxes and found that ATP-ADP exchange was faster than the calcium flux. Comparison of the calcium exchange data of Waas and Hasselbach (1981) with the nucleotide exchange of Ronzani et al. (1979) further confirms that ATP-ADP exchange is faster than calcium exchange. More recently, Takenaka et al. (1982) found in simultaneous measurements that ATP-ADP exchange was about four times as fast as calcium exchange in skeletal SR vesicles. They concluded that ATP-ADP exchange can occur without accompanying Ca-Ca exchange.

There are a number of postulated mechanisms for the Ca-ATPase of skeletal (Inesi et al., 1982; Guimaraes-Motta and DeMeis, 1980; Takakuwa and Kanazawa, 1982) and cardiac (Tada et al., 1980) SR. Each of these mechanisms invokes transitions between intermediates of the pump and many of these transitions involve binding or desorption of ligands. The mechanisms mentioned share the feature that ATP binds after outside calcium, while ADP desorbs before calcium desorbs to the internal compartment. This order of ligand sorption and desorption corresponds to Scheme A in the preceding paper (Feher, 1984). A consequence of this order of ligand sorption and desorption is that ATP-ADP exchange must exceed Ca-Ca exchange, multiplied by $1/n$, where n is the coupling ratio. Recent experiments by Ogawa and Kurebayashi (1982) suggest that the order of ligand binding in bullfrog SR is ATP first and Cao second. The relation between calcium and nucleotide exchange could then be somewhat different for bullfrog compared with rabbit skeletal SR. We have investigated nucleotide and calcium fluxes in cardiac SR to determine which ATPase reaction schemes are compatible with the experimental data.

One possible difference between cardiac and skeletal SR is the coupling ratio of calcium transport. The coupling ratio is defined as the ratio of the net rate of calcium accumulation to calcium-dependent rate of ATP hydrolysis during the steady phase of calcium uptake. This issue has been reviewed by Jones and Besch (1979). Most investigators report an apparent coupling ratio of 1 or less for cardiac SR with the exception of Tada and co-workers, who report a ratio of about 2 (Tada et al., 1974). On the other hand, the accepted coupling ratio for skeletal SR is 2. We have recently reported an average apparent coupling ratio of 0.68 mol Ca/mol ATP for cardiac SR and 1.34 for skeletal SR (Feher and Briggs, 1983). In his review, Berman (1982) indicates that nonintegral values for the coupling ratio can be explained by slippage of the pump, passive leaks or a subpopulation of incompletely sealed

vesicles. Chevallier and co-workers (1977) noted that a small population of skeletal SR vesicles (18–25%) were inactive with respect to calcium phosphate loading, but were SR vesicles by the criterion of SDS gel electrophoresis. Vesicles made hyperpermeable to calcium by adding calcium ionophores show a diminished ATP-ADP exchange but activated ATPase (Ronzani et al., 1979; Ogawa and Kurebayashi, 1982). Thus, a small population of incompletely sealed vesicles would make little or no contribution to the calcium uptake while contributing greatly to the net ATPase rate and less to the ATP-ADP exchange.

In a past report we have described methods that allow determination of unidirectional calcium fluxes attributable to the action of the pump (Feher and Briggs, 1983). In this report we combine these methods with measurements of the unidirectional nucleotide fluxes. We have corrected the fluxes for the contributions made by incompetent vesicles.

MATERIALS AND METHODS

SR Preparation

Vesicles of cardiac SR were isolated from minced canine heart as described previously (Feher and Briggs, 1982). The SR from three dogs was pooled and used for all experiments. The characteristics of these pooled preparation were calcium oxalate uptake rate, 2.07 μmol $min^{-1}mg^{-1}$, calcium oxalate capacity, 13 μmol mg^{-1}, and an apparent coupling ratio of 0.86. While this manuscript was in review, Chamberlain et al. (1983) reported on the characteristics of canine cardiac SR with "improved Ca transport properties." The Ca uptake rate of their preparation was 2.51 μmol $min^{-1}mg^{-1}$, the Ca oxalate capacity was 9.08 μmol mg^{-1}, and their coupling ratio was 0.97.

Steady State Calcium Uptake

Calcium uptake by cardiac SR vesicles was determined from a reaction bath containing 100 mM KCl, 20 mM imidazole buffer, pH 7.0, 10 mM sodium azide, 100 μM Na_2ATP, 2.1 mM $MgCl_2$ either 4 or 8 μM added calcium, 0.05 μCi, ^{45}Ca/ml, and 0.125 mg cardiac SR protein per milliliter. The cardiac SR was added 0.5 min before addition of ATP, Ca and Mg to an otherwise complete reaction bath maintained at 27°. The total calcium in the reaction bath becomes distributed among four compartments: Cao, the calcium in solution outside the vesicles; Cabo, calcium bound to the external surface of the vesicles; Cabi, calcium bound to intravesicular binding sites; and Cai, calcium free within the intravesicular space. Thus the total calcium in the reaction bath is

$$CaT = Cao + Cabo + Cabi + Cai \quad (1)$$

and the calcium associated with the SR vesicles is

$$Cat = Cabo + Cabi + Cai. \quad (2)$$

The total calcium in the reaction bath was estimated by atomic absorption spectrophotometry following extraction of the bath with trichloroacetic acid and HCl (6 and 1% final concentration, respectively). The total calcium associated with the cardiac SR was obtained following Millipore filtration and was calculated from the total ^{45}Ca in the reaction bath and ^{45}Ca in filtrates of the reaction bath.

Diffusional Passive Calcium Efflux (Jp)

Diffusional passive calcium efflux was measured after steady state calcium uptake was reached by quenching the pump-mediated calcium fluxes with 2.5 mM EGTA (ethylene glycol [*bis*-β-aminoethyl ether] N,N^1-tetraacetic acid) and observing net release of calcium by Millipore filtration. The diffusional efflux was calculated from the slope and initial values of the first-order efflux curves according to

$$Jp = (Cat - Cabo)\frac{\mathrm{d}\ln(Cat - Cabo)}{\mathrm{d}t}. \quad (3)$$

From Eq. 2 this becomes

$$Jp = \frac{\mathrm{d}(Cai + Cabi)}{\mathrm{d}t}. \quad (4)$$

The slope of the first-order efflux curve was determined by linear regression on six points obtained after EGTA quench. The initial value ($Cat - Cabo$) was determined by extrapolating the first-order efflux curve to the time of EGTA addition. The method is illustrated in Fig. 1 *B*.

Unidirectional Calcium Influx (Jf)

The total calcium influx at steady state, Jf, was estimated from the rate of ^{45}Ca-^{40}Ca exchange as previously described (Feher and Briggs, 1983). In the calcium exchange reaction, steady state calcium uptake was first achieved in a reaction bath identical to that used to measure steady state calcium uptake except ^{45}Ca was omitted. After steady state was reached, a pulse of ^{45}Ca was added and aliquots of the bath were filtered for determination of ^{45}Ca in the filtrate (Fig. 1 *A* and *C*). Jf was then calculated as described previously (Feher and Briggs, 1983).

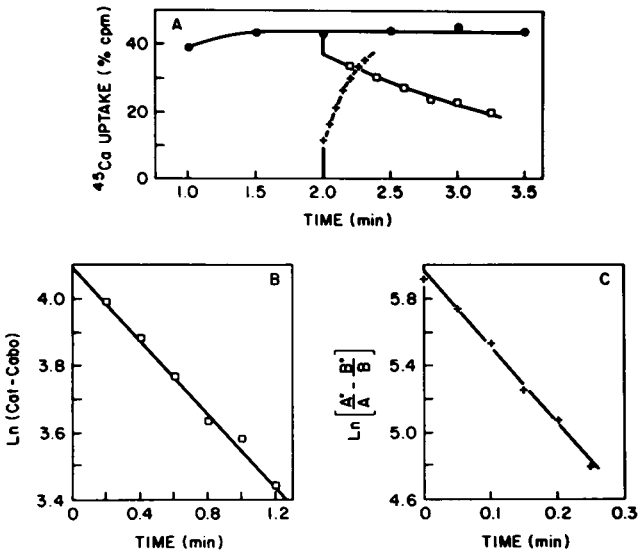

FIGURE 1 Methods for determining passive efflux and total calcium influx. ^{45}Ca distribution between cardiac SR and extravesicular calcium was determined by Millipore filtration. Steady state calcium uptake was determined by adding ^{45}Ca with unlabeled calcium at the start of the reaction (●). The passive efflux was estimated by the net efflux after adding 2.5 mM EGTA to vesicles at steady state (□). The first-order plot of efflux (*B*) was linear. Total calcium influx was estimated by adding ^{45}Ca to vesicles at steady state uptake in a bath initially containing no ^{45}Ca (+). The plot of the rate of equilibration of specific activity (*C*) gives the influx as a function of its slope. Reaction conditions were 100 mM KCl, 20 mM imidazole, pH 7.0, 10 mM sodium azide, 100 M Na_2ATP, 2.1 mM $MgCl_2$, 0.047 mg/ml cardiac SR protein, 7.5 μM total calcium by atomic absorption spectrophotometry and 27°. The meaning of A*, A, B*, and B are given in Materials and Methods section.

Pump-mediated Calcium Efflux

At steady state calcium uptake the net calcium flux is zero and total calcium influx, *Jf*, is equal to the total calcium efflux. In a previous communication (Feher and Briggs, 1983) we have shown that it is possible to partition the total efflux into a diffusional component, *Jp*, and a pump-mediated component, *Jr*. Pump-mediated calcium efflux was calculated as $Jr = Jf - Jp$, where *Jf* and *Jp* were determined as described above.

Unidirectional Nucleotide Fluxes

The unidirectional nucleotide fluxes are related by

$$JNET = JF - JR, \tag{5}$$

where *JNET* is the net nucleotide flux defined as the net rate of conversion of ATP to ADP, *JF* is the nucleotide flux in the forward direction (ATP → ADP) and JR is the reverse nucleotide flux (ATP ← ADP). The steady state *JNET* is equal to the net rate of P_i liberation from ATP.

Determination of the unidirectional nucleotide fluxes is more complicated than the unidirectional calcium fluxes because the pools of ATP and ADP are not constant. Let *A* be the pool of ATP, expressed as nmol mg^{-1}, and *B* be the ADP pool. In the region of steady state ATPase activity, the sizes of pools *A* and *B* are given by

$$A = -JNET\,(t - t_1) + A_1 \tag{6}$$

$$B = JNET\,(t - t_1) + B_1, \tag{7}$$

where *JNET* is the net rate of conversion of ATP to ADP, in nanomoles per minute per milligram, and A_1 and B_1 are the sizes of pools *A* and *B*, respectively, at some time t_1. The unidirectional fluxes between *A* and *B* can be estimated by a pulse label of nucleotide into either pool. If A^* is the amount of ^{3}H-ATP nucleotide in pool *A* and B^* the amount of ^{3}H-ADP in pool *B*, then

$$\frac{dA}{dt} = -JF\frac{A^*}{A} + JR\frac{B^*}{B}, \tag{8}$$

where *A* and *B* are the linear functions of time given in Eqs. 6 and 7. In addition, we require the conservation relations

$$A + B = A_0 \tag{9}$$

$$A^* + B^* = B_0^*, \tag{10}$$

which state that the total amount of nucleotide is conserved and that the pulse label was added as ADP. These equations (6–10) can be used to derive an expression for *JR*

$$JR = -JNET\frac{\ln\,[1 - A_0A_2^*/B_0^*A_2]}{\ln\,[A_1B_2/A_2B_1]}, \tag{11}$$

where A_1 and B_1 are the values of *A* and *B* at time t_1 when the pulse label was added and A_2, B_2, and A_2^* are the values of *A*, *B*, and A^* at some time t_2 after addition of the pulse label. Note that there is no plot that will give *JR* as a function of its slope. Values for *JR* are calculated for each set of values of *A*, *B*, and A^* determined after addition of pulse label. Time does not appear explicitly in the equation but remains incorporated into its result through the equations describing *A* and *B* as functions of time.

In a similar way an expression for *JF* may be derived

$$JF = JNET\frac{\ln\dfrac{B_1}{B_2}\dfrac{(A_2^* - A_0^*A_2/A_0)}{(A_1^* - A_0^*A_1/A_0)}}{\ln\,[A_2B_1/B_2A_1]}, \tag{12}$$

where the variables have the same meaning as before. The formulae for *JF* and *JR* are not symmetrical because in the derivation of *JR* it was assumed that the pulse label of [^{3}H]ADP was free of [^{3}H-ATP]. This can be experimentally verified as described below. The pulse label of [^{3}H]-ATP, however, usually contains some [^{3}H]-ADP. Thus, the total radioactivity added A^*_0, is not equal to A^*_1, the radioactivity present in the ATP pool at the time of addition of the pulse label.

As with *JR*, *JF* was determined from an average of six points obtained from a single reaction bath. Representative values for *JF* and *JR* for a particular condition are given in Table I. The average coefficient of variation was 6.7% for *JR* and 8.5% for *JF* for 13 determinations like the single determination shown in Table I.

The values of A_1, B_1, *A*, and *B* necessary to use Eqs. 11 and 12 can be obtained from A_i and B_i, the initial sizes of *A* and *B*, and the net rate of conversion of ATP to ADP, *JNET*. The total nucleotide, A_0, was checked by the absorbance at 259 nm using the molar extinction coefficient $\epsilon_m = 15.4 \times 10^3$ (Bock et al., 1956). The initial ADP contamination was estimated by the decrease in absorbance at 340 nm when ADP was coverted to ATP by the coupled enzyme system of pyruvate kinase and lactate dehydrogenase (Warren et al., 1974). *JNET*, *JF*, and *JR* were determined from three identical baths. For determination of *JNET*, [2,8-^{3}H]-ATP (New England Nuclear, Boston, MA; 28 Ci/mmol) was added (10 μCi/ml) with ATP, Ca, and Mg to begin the reaction. For determination of *JF*, the same procedure was followed except [^{3}H]-ATP was added after steady state ATP hydrolysis and calcium uptake were reached. The time of addition of [^{3}H]-ATP was the same as the time at which calcium exchange was measured. For estimation of *JR*, the same procedure was followed as for *JF* except [2,8-^{3}H]-ADP (New England Nuclear, 30 μCi/mmol) was added in place of [^{3}H]-ATP. At various times after addition of [^{3}H]-ATP or [^{3}H]-ADP, the reaction was quenched by adding 50 μl of reaction bath to 50-μl chilled 10% trichloroacetic acid. The mixture was then neutralized with 32 μl 1 N NaOH and 25 μl of nucleotide carrier (30 mM ATP, 30 mM ADP, 30 mM AMP) was added. The nucleotide fractions of a 5-μl aliquot of this mixture were separated by thin-layer chromatography on polyethyleneimine-cellulose plates (Merck, Darmstadt, Federal Republic of Germany) developed with 2 N formic acid, 0.5 M LiCl (Suko and Hasselbach, 1976; Verjovski-Almeida et al., 1978). The spots of ATP, ADP, and AMP were located under ultraviolet light, scraped off the plastic support, and extracted with 1.0 ml of 0.7 M $MgCl_2$ in 20 mM imidazole buffer, pH 7.0. The extracted nucleotides were solubilized with 10-ml chilled Biofluor (New England Nuclear) and counted by liquid scintillation spectrometry.

TABLE I
DETERMINATION OF UNIDIRECTIONAL NUCLEOTIDE FLUXES

Time after pulse label	*JF*	*JR*
min	*nmol min^{-1} mg^{-1}*	*nmol min^{-1} mg^{-1}*
0.2	298	166
0.4	250	171
0.6	233	171
0.8	280	178
1.0	257	170
1.2	294	168
	$\bar{x} = 269 \pm 11$	$\bar{x} = 170 \pm 2$

Unidirectional forward nucleotide flux (*JF*) and reverse nucleotide flux (*JR*) were determined by adding [^{3}H]-ATP or [^{3}H]-ADP, respectively, to reaction baths that had obtained steady state calcium uptake and ATPase activity. The reaction bath contained 100 mM KCl, 20 mM imidazole, pH 7.0, 10 mM NaN_3, 100 μM ATP, 2.1 mM $MgCl_2$, 7.5 MM $CaCl_2$, 0.047 mg cardiac SR protein per milliliter and 4 μM EGTA. *JF* and *JR* were calculated from the ^{3}H counts per minute in the ATP and ADP fractions according to Eqs. 11 and 12.

For the above methods to be valid, we require that the three reaction baths used to determine *JNET*, *JF*, and *JR* be identical. If they are identical, then the distribution of counts between ATP and ADP will asymptotically approach the same value for all three baths. This requirement can be met (Fig. 2 *A*). Normally the values of *JF* and *JR* are calculated in a region of the curves in which JNET is steady (Fig. 2 *B*).

The ATP ← ADP flux due to SR Ca-ATPase can be overestimated due to the activity of contaminating adenylate kinase. We evaluated this by the rate of ^3H incorporation into AMP by routinely counting the AMP fraction after thin-layer chromatography (Kurebayashi et al., 1980). The results indicate that the ATP ← ADP flux due to adenylate kinase was small. In any case, the adenylate kinase activity would contribute fully to the calcium-independent *JR* (Kurebayashi et al., 1980), which was subtracted from the total *JR* to obtain the calcium-dependent reverse nucleotide flux. In this way contributions of adenylate kinase were corrected.

We have used [^3H]-ATP or [^3H]-ADP entirely in these studies because [γ-^{32}P]-ATP obtained commercially often cannot be completely hydrolyzed. The fraction that cannot be hydrolyzed increases with time of storage. We therefore had little confidence in calculations of *JNET* based on the rate of [^{32}P]-ATP hydrolysis because the specific activity of the ATP was in doubt.

Correction for Nucleotide Fluxes by Incompetent Vesicles

Since the aim of the study was to compare unidirectional calcium and nucleotide fluxes in the same vesicles, it was necessary that the vesicles be homogeneous. We recognized the probability that our preparation was not homogeneous and made a correction for the heterogeneity. We assumed that our preparation was a mixture of vesicles that were either fully competent or fully incompetent, where incompetent means incapable of accumulating calcium. The unidirectional calcium fluxes are those fluxes that occur in competent vesicles only and incompetent vesicles do not contribute to the measured calcium fluxes. However, the incompetent vesicles do contribute to the observed unidirectional nucleotide fluxes. If f_c is the fraction of cardiac SR protein in the competent vesicles and f_i the fraction in incompetent vesicles, then

$$JNET = f_cJNET_c + f_iJNET_i \quad (13)$$

$$JF = f_cJF_c + f_iJF_i \quad (14)$$

$$JR = f_cJR_c + f_iJR_i \quad (15)$$

where *JNET* is the overall net nucleotide flux, in nanomoles per minute per milligram, and *JF* and *JR* are the similar unidirectional nucleotide fluxes; $JNET_c$ is the specific activity, in nanomoles per minute per milligram, of the net nucleotide flux of the competent vesicles; $JNET_i$ is the specific activity of the net nucleotide flux of incompetent vesicles; JF_c, JR_c, JF_i, and JR_i are the specific activities of the unidirectional nucleotide flux of competent and incompetent vesicles, respectively. The nucleotide fluxes contributed by the competent vesicles are f_cJNET_c, f_cJF_c, and f_cJR_c, and these values are to be compared with *Jp*, *Jf*, and *Jr*, the reverse pump-mediated calcium flux. The quantities measured by our methods are *JNET*, *JF*, and *JR*. We calculated f_cJNET_c, f_cJF_c, and f_cJR_c by separately determining $f_c = 1 - f_i$ and $JNET_i$, JF_i, and JR_i, and inserting their values into Eqs. 13–15.

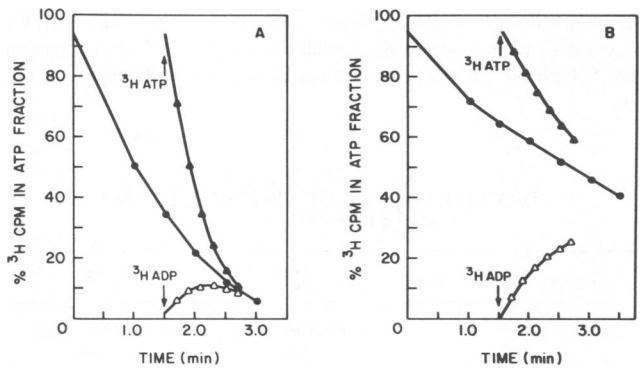

FIGURE 2 Methods for determining unidirectional nucleotide fluxes. Reaction conditions were 100 mM KCl, 20 mM imidazole, pH 7.0, 10 mM sodium azide, 100 M Na_2ATP, 2.1 mM $MgCl_2$, 0.125 mg/ml cardiac SR protein and (*A*) 15.2 μM total calcium or (*B*) 11.2 μM total calcium plus 4 μM EGTA. The net ATPase rate (*JNET*) was determined by adding [^3H]-ATP at the beginning of the reaction (●). The forward nucleotide flux (*JF*) was estimated from the curve obtained after adding [^3H]-ATP when steady state ATP hydrolysis was reached (▲). The reverse nucleotide flux was estimated from the curve obtained when [^3H]-ADP was added during steady state ATP hydrolysis (△). The confluence of curves in *A* indicates the three reaction baths were in agreement, but the *JNET* is not sufficiently linear for useful data to be obtained. Fluxes were more usually analyzed during a steady state region of ATP hydrolysis (*B*).

The nucleotide fluxes of competent and incompetent vesicles in a single bath are linked by the fact that the two types of vesicles are in contact with the same solution containing definite concentrations of ATP, ADP, and Ca_o. The values of $JNET_i$, JF_i and JR_i were determined by making all vesicles incompetent by adding 2 μM A23187 (generously supplied by Dr. R. Hamill, Eli Lilly Co., Indianapolis, IN). This concentration of calcium ionophore precludes any calcium uptake by rapidly dissipating any calcium gradient. The values of $JNET_i$, JF_i, and JR_i in the mixture of competent and incompetent vesicles was determined by interpolation to the value of pCa obtained during steady state calcium uptake. The concentrations of ATP and ADP were comparable when these interpolations were made.

The fraction of competent vesicles was determined by estimating the fraction of SR protein that could be loaded with calcium oxalate under maximal loading conditions. Vesicles loaded with calcium oxalate were separated from unloaded vesicles by centrifugation through 40% surcose for 30 min at 100,000 *g*. The maximal capacity of cardiac SR for calcium oxalate was initially determined using a low protein concentration, 0.015 mg/ml, under conditions specified in the legend to Fig. 6. In the experiment to determine fractional competence, the SR was loaded under significantly different conditions because it was necessary to load larger quantities of SR protein. In this experiment, 3.86 mg of SR protein was added to a 20-ml bath at 37° containing 100 mM KCl, 20 mM imidazole buffer, pH 7.0, 10 mM sodium azide, 5 mM ATP, 5 mM $MgCl_2$, 10 mM K oxalate, 0.2 mM $CaCl_2$, and 0.05 μCi 45 Ca/ml. At 1 min, and approximately at 2-min intervals thereafter, 100 μl aliquots of the reaction mixture was assayed for calcium uptake by Millipore filtration. At 2 min, and approximately at 2-min intervals thereafter, 1.6 μmol of $^{45}CaCl_2$ of identical specific activity was added per milligram of SR protein. After 9 min of incubation, 100 μmol of ATP was added. A total of seven additions of calcium were made before calcium uptake plateaued. At this point the loading was considered complete. The calcium oxalate load of this point was 11.2 μmol mg^{-1} SR protein. After centrifugation through 40% sucrose, the recovered pellets and supernatant phase were assayed for total protein and ATPase activity in the presence of 2 μM A23187 by a colorimetric method (King, 1932).

RESULTS

The dependence of the specific activities of the net and unidirectional nucleotide fluxes on the extravesicular free-calcium concentration is shown in Figs. 3 and 4. When the calcium ionophore, A23187, is added to the vesicles, there is a marked elevation in the net nucleotide flux that is associated with an increase in the forward nucleotide flux

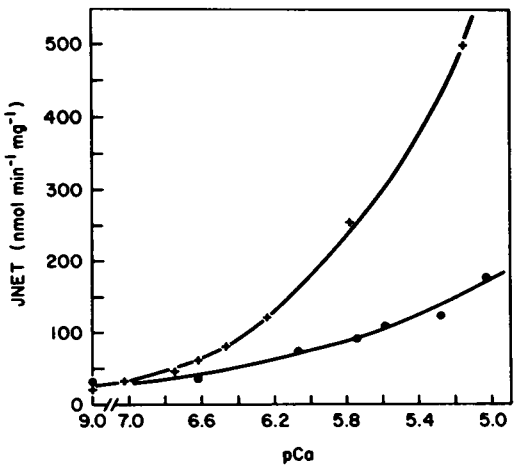

FIGURE 3 Net ATPase activity as a function of free extravesicular calcium concentration in the presence (+) and absence (●) of 2 μM A23187. Reaction conditions were identical to those described in the legend to Fig. 2 except that 0–5 mM EGTA was added to vary the extravesicular calcium.

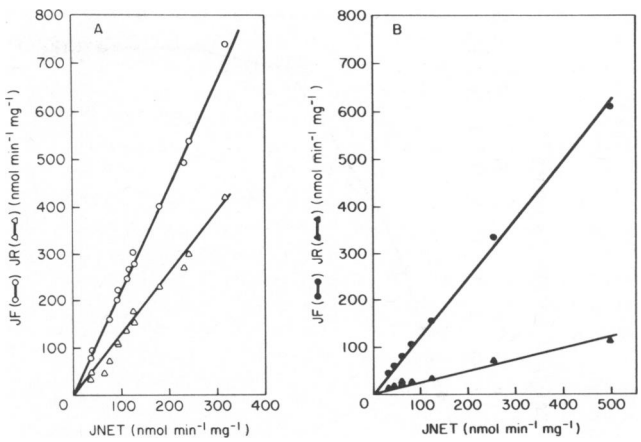

FIGURE 5 Relation between unidirectional nucleotide fluxes and net ATP hydrolysis in native vesicles (*A*) and vesicles made hyperpermeable by addition of A23187 (*B*). Data for *A* were the composite values for three separate cardiac SR preparations. Conditions were similar to those for Figs. 2–4 except total calcium and protein concentrations were slightly different.

and a decrease in the reverse nucleotide flux. At any given pCa, the net and forward nucleotide fluxes are increased by A23187, while the reverse nucleotide flux is diminished. This is the expected result as shown in the previous communication and agrees with previous reports (Ogawa and Kurebayashi, 1982). In Fig. 5, the specific activities of the unidirectional nucleotide fluxes are plotted against the specific activity of the net nucleotide flux for native vesicles and for vesicles made hyperpermeable by addition of A23187. The data in Figs. 3–5 indicated that a small quantity of hyperpermeable vesicles in the native vesicles could alter considerably the ratio JF/JR and could make a significant contribution to $JNET$. Since these vesicles would not contribute to the calcium fluxes, the overall ratio of calcium and nucleotide fluxes would be in error.

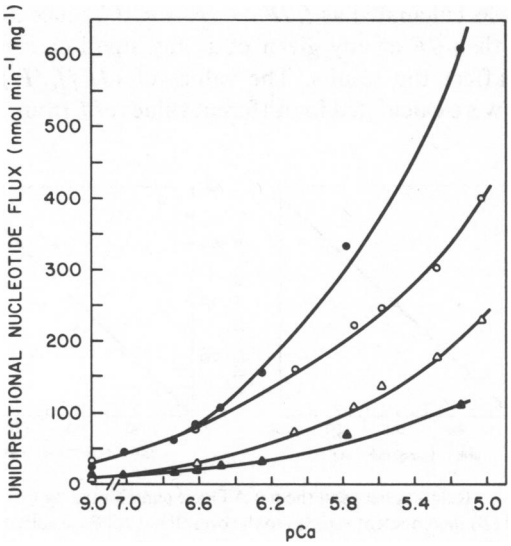

FIGURE 4 Unidirectional forward (●, ○) and reverse (▲, △) nucleotide fluxes as a function of free extravesicular calcium concentration in the presence (●, ▲) and absence (○, △) of A23187. Reaction conditions as described in Figs. 2 and 3.

To determine the nucleotide fluxes associated with calcium fluxes, JF_i, JR_i, and $JNET_i$ had to be determined for incompetent SR and the fraction of SR that is incompetent (f_i) had to be established. The specific activities of JF_i, JR_i, and $JNET_i$ are presented as a function of pCa in Figs. 3 and 4. The fraction of competent vesicles was estimated by loading native vesicles to capacity and then centrifuging the loaded vesicles through 40% sucrose. The rate and extent of maximal loading is shown in Fig. 6. The initial rate of loading was ~2 μmol $min^{-1}mg^{-1}$ and the capacity was 13 μmol mg^{-1}. These rates and capacities compare favorable with those reported by others (Levitsky et al., 1976; Jones and Cala, 1981) and suggest the vesicles represent a fairly homogeneous population. The fraction of the vesicle protein that would sediment through 40% sucrose is shown in Table II. Three experimental conditions were investigated. Control SR was not subjected to experimental manipulation. The augmented vesicles were loaded with calcium oxalate and layered over 40% sucrose. The nonaugmented vesicles were incubated in the absence of oxalate and then layered over 40% sucrose. Augmented and nonaugmented vesicles were centrifuged at 30,000 *g* for 30 min. The data in Table II show that none of the protein in the nonaugmented vesicles sedimented through 40% sucrose, very little calcium-dependent ATPase activity was lost and protein recovery was nearly complete. For the augmented vesicles recovery of protein was 87% and recovery of ATPase activity was 72%. Of the protein recovered, 86% sedimented through 40% sucrose. Of the ATPase activity recovered, 88% sedimented through 40% sucrose. On the basis of this data, ~86% of the SR is sufficiently competent to generate the calcium gradient needed to accumulate calcium oxalate. Although the spe-

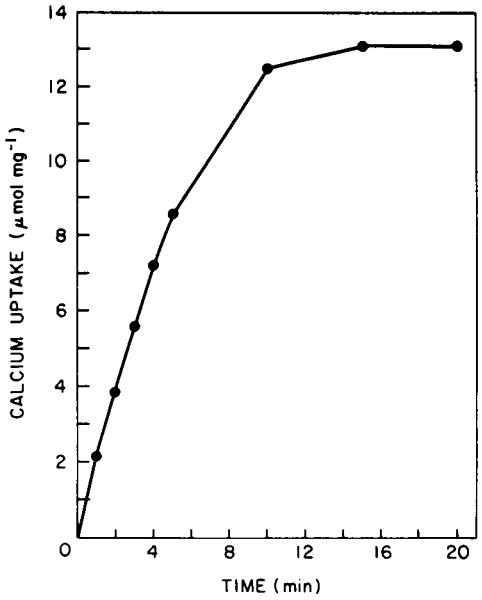

FIGURE 6 Capacity of cardiac SR. Vesicles were loaded in a medium containing 0.0125 mg/ml cardiac SR protein, 100 mM KCl, 20 mM imidazole buffer, pH 7.0, 10 mM sodium azide, 5 mM ATP, 5 mM $MgCl_2$, 10 mM K oxalate, 0.2 mM calcium, and 0.05 Ci ^{45}Ca/ml maintained at 37°. Calcium uptake was determined by counting aliquots of the filtrate following Millipore filtration.

cific activities of the ATPases of the heavy and light fractions of augmented vesicles are slightly different, they are similar enough to believe that the light fraction is incompetent SR. Chevallier and co-workers (1977) reached the same conclusion for phosphate-loaded SR on the basis of morphology and protein composition. Another justification for this estimate of competency was the apparent coupling ratio for the native vesicles. In the presence of 10 mM oxalate, the ratio of calcium uptake to Ca-dependent ATPase activity was 0.86. Since in the presence of oxalate the Ca-dependent ATPase is the same for competent and incompetent cardiac SR (Feher and Briggs, 1980), it follows that an assumed coupling ratio of 1:1 is consistent with a fractional competency of 0.86.

TABLE II
EFFECT OF DENSITY AUGMENTATION BY CALCIUM-OXALATE LOADING ON SEDIMENTATION OF SR THROUGH 40% SUCROSE

Preparation	Protein		Ca-ATPase		Percent recovered
	Total	Percent recovered	Total	Specific activity	
	mg		*μmol min⁻¹*	*μmol min mg⁻¹*	
Control SR	4.03	100	8.34	2.07	100
Nonaugmented SR (light fraction)	4.10	102	8.12	1.98	97
Augmented SR (light fraction)	0.48	12	0.72	1.52	9
(heavy fraction)	3.04	75	5.29	1.74	63
Total of augmented SR fractions	3.52	87	6.01	1.71	72

Calcium-oxalate loading was performed as described in Methods. ATPase activity was measured in the presence of the calcium ionophore, A23187, as described in Methods.

At this point the values of $JNET$, JF, JR, $JNET_i$, JF_i, and JR_i were available as a function of pCa (Figs. 3 and 4 and $f_c = 0.86$ and $f_i = 1 - f_c = 0.14$ were estimated. After interpolation on the pCa curves, we used Eqs. 13–15 to calculate f_cJF_c, f_cJR_c, JF_c, and JR_c. Here f_cJF_c and f_cJR_c are the unidirectional nucleotide fluxes contributed by competent vesicles, and JF_c and JR_c are the specific activities of these fluxes in the competent vesicles. When the values of $JNET_c$, JF_c, and JR_c were calculated, it was found that the ATPase rate in the mixture of competent and incompetent vesicles was about equally contributed by competent and incompetent vesicles (Fig. 7). In other words, half of the ATPase at steady state calcium uptake was due to vesicles that did not accumulate calcium. This result was due to the greater specific activity of the incompetent vesicles (Fig. 8) at any given $JNET$. The unidirectional nucleotide fluxes in competent vesicles were linearly related to the net nucleotide flux in these vesicles as shown in Fig. 9.

The relations between Jf and f_cJF_c and Jr and f_cJR_c are shown in Fig. 10. In both cases the unidirectional calcium fluxes were linearly related to their respective unidirectional nucleotide flux. The slopes of the lines shown were $Jf = 1.30 f_cJF_c$ and $Jr = 1.43 f_cf_cJR_c$. Linear regression on all five points gave slopes of 1.72 and 1.90 for forward and reverse unidirectional fluxes, respectively. These results suggest that the ratio of unidirectional flux ratios, $(Jf/f_cJF_c)/(Jr/f_cJR_c)$ will be close to unity. The calculation of this ratio depends upon the value of $f_i = 1 - f_c$. The measured fluxes were JF, JR, JF_i, and JR_i. The value of f_cJF_c was calculated as $f_cJF_c = JF - f_iJF_i$. Since JF_i was larger than JF at any given pCa, any small change in f_i could affect the results. The values of $(JF/f_cJF_c)/(Jr/f_cJR_c)$ were calculated for different values of f_i from zero to

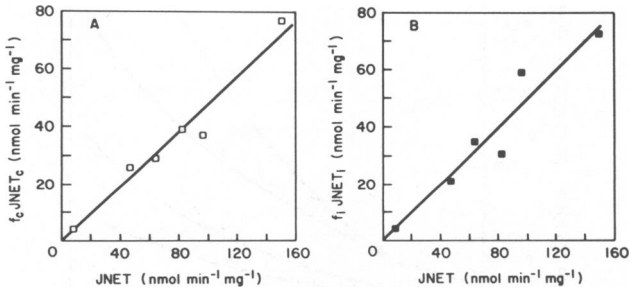

FIGURE 7 Relation between the net ATPase contributed by (*A*) competent and (*B*) incompetent vesicles to the overall net ATPase activity of the mixture of vesicles present in the native cardiac SR preparation. Data are from Fig. 3. The Ca-independent activities have been subtracted and f_i was 0.14. The values of f_iJNET_i were calculated from f_i and the interpolated value of $JNET_i$ from Fig. 3. The values of f_cJNET_c were calculated as $JNET - f_iJNET_i$.

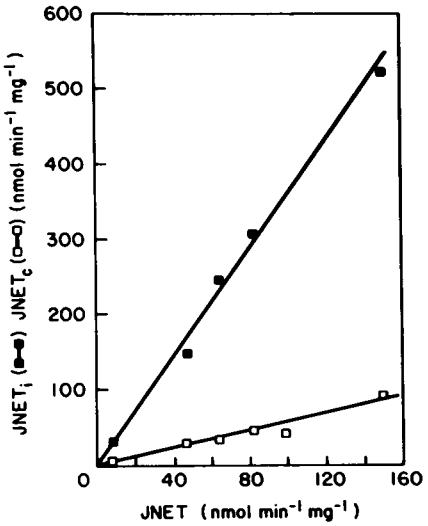

FIGURE 8 Relation between the specific activities of ATPase rate in competent ($JNET_c$) and incompetent ($JNET_i$) vesicles and overall ATPase rate in the mixture of vesicles ($JNET$). The values of $JNET_i$ were the interpolated values from Fig. 3 and $JNET_c$ was calculated as $(JNET - f_iJNET_i)/(1 - f_i)$, where f_i was 0.14.

0.20. The average values of $(Jf/f_cJF_c)/(Jr/f_cJR_c)$ are shown in Table III. The ratio of ratios was always <1 but the average was significantly <1 only when $f_i \leq 0.16$. Our experimental estimate of f_i was 0.14.

During steady state calcium uptake the incompetent vesicles made a significant contribution to the observed

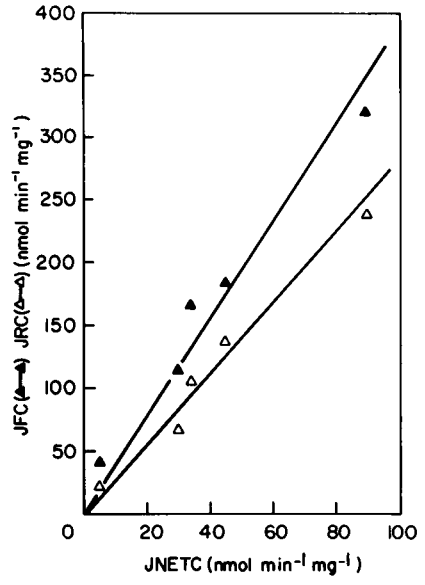

FIGURE 9 Relations between unidirectional and net nucleotide fluxes in competent vesicles. $JNET_c$ was calculated as described in the legend to Fig. 8. JF_c and JR_c were calculated in an analogous way as $(JF - f_iJF_i)/(1 - f_i)$ and $(JR - f_iJR_i)/(1 - f_i)$, where JF and JR were the observed unidirectional nucleotide fluxes at specified pCa from Fig. 4, JF_i and JR_i were the specific activities of the forward and reverse nucleotide fluxes in hyperpemeable vesicles, from Fig. 4, and $f_i = 0.14$ was the fraction of incompetent vesicles.

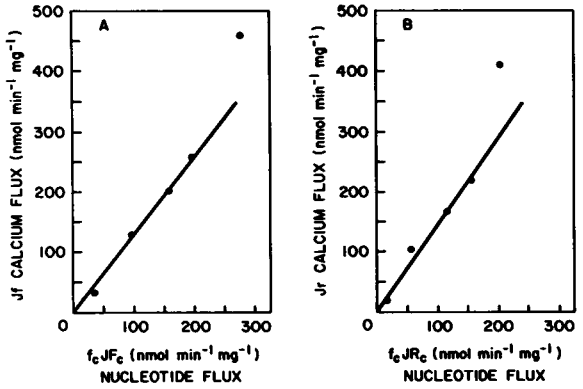

FIGURE 10 Relation between unidirectional pump-mediated calcium and nucleotide fluxes in competent vesicles. Pump-mediated calcium influx, Jf, and efflux, Jr, were determined as described in Methods. The unidirectional nucleotide fluxes contributed by competent vesicles were calculated as $f_cJF_c = JF - f_iJF_i$ and $f_cJR_c = JR - f_iJR_i$, where JF and JR were the observed forward and reverse nucleotide fluxes at specified pCa from Fig. 4, JF_i and JR_i were the specific activities of the forward and reverse nucleotide fluxes in incompetent vesicles at the same specified pCa, from Fig. 4, and $f_i = 0.14$ was the fraction of incompetent vesicles.

$JNET$ (see Fig. 7). This raises the possibility that at steady state the passive calcium efflux, Jp, may be perfectly balanced by an opposing net calcium flux $(Jf - Jr)$, which is stoichiometrically coupled to the net nucleotide flux mediated by the calcium pump. The results, shown in Fig. 11, support this view. The line drawn on this graph corresponds to a fixed stoichiometry of 1 mol Ca to 1 mol ATP hydrolyzed. The data are insufficiently precise to determine whether the stoichiometry is fixed or is an integer.

DISCUSSION

The results reported in this study bear upon five issues: (*a*) homogeneity of SR preparations; (*b*) competency of the

TABLE III
RATIO OF UNIDIRECTIONAL FLUX RATIOS FOR CARDIAC SR FOR VARYING FRACTIONAL COMPETENCY

f_i	$(Jf/f_cJF_c)/(Jr/f_cJR_c)$	t statistic	
0	0.64 ± 0.02	18.2	$P < 0.005$
0.07	0.75 ± 0.07	3.74	$P < 0.01$
0.14	0.87 ± 0.04	3.25	$P < 0.02$
0.16	0.90 ± 0.04	2.34	$P < 0.05$
0.18	0.93 ± 0.04	1.49	—
0.20	0.97 ± 0.05	0.72	—

Unidirectional pump-mediated calcium influx (Jf) and efflux (Jr) were determined as described in Methods. f_cJF_c was calculated as $JF - f_iJF_i$ and f_cJR_c was calculated as $JR - f_iJR_i$, where JF and JR were the unidirectional forward and reverse nucleotide fluxes, respectively, for native vesicles and JF_i and JR_i were the unidirectional forward and reverse nucleotide fluxes for vesicles made incompetent by adding the calcium ionophore A23187. The values reported for $(Jf/f_cJF_c)/(Jr/f_cJR_c)$ are the mean ± SEM, $n = 5$. The t statistic tests the null hypothesis that $(Jf/f_cJF_c)/(Jr/f_cJR_c) \geq 1.0$. The critical value of the t statistic for a one-tailed t test with $P \leq 0.05$ is 2.13.

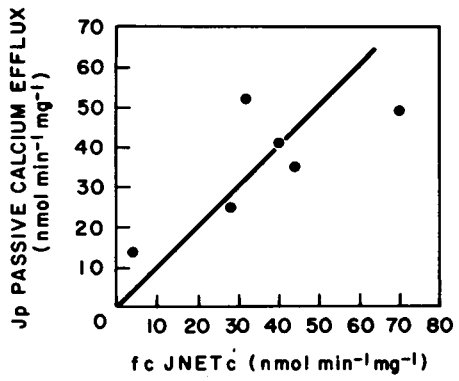

FIGURE 11 Coupling of net calcium flux to net ATPase hydrolysis in competent vesicles. The net calcium flux ($Jp = Jf - Jr$) mediated by the calcium pump at steady state was evaluated as the parallel passive efflux obtained by EGTA quench after attainment of steady state uptake. The net ATPase activity of incompetent vesicles was determined as described in the legend of Fig. 9. Reaction conditions were those described in the legend of Fig. 2. The line shown represents a stoichiometry of 1 mol calcium transported per mole ATP hydrolyzed.

SR; (*c*) apparent coupling ratios; (*d*) order of binding and desorption of ATP, ADP, and Ca, and (*e*) stoichiometry of the calcium pumps in cardiac SR.

Homogeneity

Homogeneity of the SR preparations is necessary for the unambiguous interpretation of kinetic data. The vesicles could be heterogeneous with respect to size, internal calcium-binding proteins, protein/lipid ratio, lipid composition, protein composition, sensitivity to some agents, and contamination by vesicles from another membrane such as the sarcolemma. Jones and Cala (1981) reported that their crude dog cardiac SR preparation contained subpopulations that varied in their sensitivity to ryanodine. When their preparation was loaded with calcium oxalate and subjected to sucrose gradient centrifugation, 12% of the protein contained 8 μmol mg^{-1} calcium oxalate, while the overall load was only 0.9 μmol mg^{-1} calcium oxalate. The vesicles containing 8 μmol mg^{-1} calcium oxalate could be further loaded to a total of ~12 μmol mg^{-1} and this loading was insensitive to ryanodine. The unloaded vesicles, which constituted the major portion of crude SR protein, could take up ~4 μmol mg^{-1} calcium oxalate in the presence of ryanodine. Levitsky and co-workers (1976) report that dog cardiac SR isolated by sucrose gradient centrifugation after calcium oxalate loading will accumulate ~15 μmol mg^{-1}. Our dog cardiac SR preparation, without previous loading with calcium oxalate, had a capacity of 13 μmol mg^{-1} (see Fig. 6), and 86% of the recovered protein was recovered in the calcium-loaded fraction. The capacity of our SR preparation is 0.86 times that of SR from Levitsky and co-workers (1976), suggesting that competent SR vesicles are comparable between our two laboratories.

Kinetic criteria for homogeneity of vesicles has been described by Hopfer (1981). According to Hopfer's view, if the isotope exchange of transported ligand across the membrane obeys a single exponential at two different conditions, then homogeneity of vesicles may be assumed. We have observed that Ca_o-Ca_i exchange obeys a single exponential (see Fig. 1) and that a single exponential is observed when pCa is varied from 6.6 to 5.0, where the rate of exchange varies markedly. The observations that exchange obeys a single exponential and that the major portion of the vesicles load with calcium oxalate suggest that the cardiac SR preparation we used was functionally homogeneous. Our preparation may, however, represent some subpopulation of the total myocardial SR.

Competency of the Isolated Cardiac SR

It is assumed in the analysis of the data that the nucleotide fluxes that occur between states of the enzyme are accompanied by calcium fluxes. This assumption is made for the incompetent as well as the competent vesicles. The problem is that the calcium fluxes are not expressed in incompetent vesicles because incompetent vesicles do not accumulate calcium. Therefore, the nucleotide fluxes associated with these nonexpressed calcium fluxes must be subtracted from the total nucleotide fluxes before associations between nucleotide and calcium fluxes can be made. Only totally incompetent vesicles are of concern because it is only these vesicles in which calcium fluxes cannot be measured. We have identified these vesicles by their inability to produce a calcium gradient sufficient to induce oxalate crystallization, i.e., by their inability to load with calcium oxalate. The fraction of vesicles that we found incompetent by oxalate loading was 14%, a value similar to the 15–25% reported by Chevallier et al. (1977) for skeletal SR using phosphate loading to augment SR density.

If we have overestimated the fraction of incompetent vesicles, then we have overestimated $(Jf/f_cJF_c)/(Jr/f_cJR_c)$, see Table III. We know from Fig. 1 of Feher and Briggs (1980) that A23187 at a concentration of 0.3 μM does not completely block calcium accumulation but does completely block calcium oxalate accumulation. Thus SR that can produce only a small calcium gradient is judged incompetent by the oxalate loading method. The ratio of $(Jf/f_cJF_c)/(JR/f_cJR_c)$ is, therefore, somewhat overestimated. In terms of the decision about the sequence of adsorption and desorption of calcium and nucleotides, the above-mentioned ratio is conservative since a lower value of the ratio has a greater significance.

Apparent Coupling Ratios

The apparent coupling ratios Jf/f_cF_c and Jr/f_cJR_c were 1.27 and 1.48, respectively (Fig. 10), for cardiac SR. These ratios are apparent coupling ratios in the best sense for they represent unidirectional fluxes in competent vesicles only. Analyses of the origin of these ratios in the preceding paper (Feher, 1984) indicates that they need not be integers nor

are they necessarily constant. They are not necessarily integers because the unidirectional nucleotide and calcium fluxes occur over different sets of intermediates.

The ratio of Jr/f_cJR_c for cardiac *SR*, 1.43, is strikingly different from the ratio Jr/JR of 0.172, which can be calculated from the data of Ronzani et al. (1979) and Waas and Hasselbach (1981) or the ratio of 0.188 reported by Takenaka et al. (1982) for skeletal SR. The ratio Jr/f_cJR_c was chosen for comparison because JR is not greatly affected by the presence of incompetent SR (Fig. 4). The values of *Jr* in this study ranged from 20–400 nmol min^{-1} mg^{-1}, depending upon conditions, and are similar to those reported by Waas and Hasselbach (1981), 310 nmol min^{-1} mg^{-1}, and Takenaka et al. (1982), 245 nmol min^{-1} mg^{-1} for skeletal SR. The difference in the ratio of Jr/JR in cardiac as compared with skeletal SR is due to the much greater *JR* in skeletal muscle as compared with cardiac muscle when ATP and ADP are the nucleotides involved in exchange. When the ratio Jr/JR is calculated from the papers by Ronzani et al. (1979) and Waas and Hasselbach (1981) for GTP and GDP as substrates, a ratio of 1.18 is obtained. Thus the numerical values for Jr/JR depend both on the source of the SR and the nucleotide supporting calcium transport.

Waas and Hasselbach (1981) and Takenaka et al. (1982) conclude that a large reverse nucleotide flux must take place independent of calcium flux because the ratio of these fluxes exceeded 2 by a considerable factor. In reaching this conclusion these authors failed to take into consideration that the calcium and nucleotide fluxes do not occur over identical set of intermediates. Their data is, in fact, compatible with Scheme A of Feher (1984).

Order of Binding and Desorption of ATP, ADP, and Ca

For a reaction cycle with no branched pathways, the ratio of unidirectional calcium and nucleotide flux in either direction or the ratio of these ratios in the forward and reverse directions can be used to evaluate various sequences. The following four sequences are considered by Feher (1984).

Scheme A:	Cao	ATP	ADP	Cai
Scheme B:	Cao	ATP	Cai	ADP
Scheme C:	ATP	Cao	ADP	Cai
Scheme D:	ATP	Cao	Cai	ADP
	1	2	3	4	5

The ratio Jr/JR must be less than or equal to *n*, the coupling ratio, for Scheme A. For Scheme D, Jr/JR must be greater than or equal to *n*. For skeletal SR, where *n* is apparently 2 (see Berman, 1982, for review), Scheme A is compatible with the values calculated above for Jr/JR. For cardiac SR, where *n* may be 1 (Chamberlain et al., 1983), Schemes B, C, and D are compatible with the observed value of Jr/f_cJR_c.

The value of $(Jf/f_cJF_c)/(Jr/f_cJR_c)$ also varies with the binding sequence considered. Sequence A requires $(Jf/f_cJF_c)/(Jr/f_cJR_c) > 1.0$, while sequence D requires $0 < (Jf/f_cJF_c)/(Jr/f_cJR_c) < 1.0$. The value of the ratio of ratios for sequences B and C could be either < 1 or > 1. The observation was that $(Jf/f_cJF_c)/(Jr/f_cJR_c)$ was < 1 (see Table II). From this we also infer that sequence A is not a possible description of the mechanism of the Ca pump in cardiac SR. Sequence B and D are not likely because they require that Ca desorb before ADP. Evidence against this possibility is reviewed in the preceding paper (Feher, 1984). Sequence C is thus the only linear sequence compatible with the data and distinguishes cardiac SR from skeletal SR, where sequence A is the most probable linear sequence.

The reaction sequences we have considered are clearly simplifications of the actual reaction mechanisms. Random binding of ATP, Cao, and desorption of Cai and ADP would provide all four binding sequences in a single mechanism. The observed ratio of ratios would then suggest that sequence A was followed less often than C in cardiac SR.

Stoichiometry of the Calcium Pump

The term coupling ratio should be reserved for the ratio of net fluxes. The coupling ratio of the calcium pump would be the net calcium flux mediated by the pump divided by the net ATPase mediated by the pump in competent vesicles. At steady state calcium uptake, the total net calcium flux is zero. This is the result of a balance between net calcium influx by the pump and passive calcium leak parallel to the pump. In previous publications (Feher and Briggs, 1982; 1983) we have documented that the passive efflux, *Jp*, at steady state can be evaluated as the initial efflux after EGTA quench of the Ca-ATPase activity. Hara and Kasai (1977) measured calcium efflux from skeletal SR in this way and compared it with the total Ca-ATPase activity. If the coupling ratio were 2.0, then *JNET* should be ½ *Jp*. The observed *JNET* was much larger than ½ *Jp*, and, in fact, was usually much larger than *Jp*. We have also observed that *JNET* is usually much larger than *Jp* in cardiac SR vesicles. Berman addresses this issue in his review (Berman, 1982) in which he indicates that the nonintegral values of calcium uptake rate/ATP hydrolysis rate can be explained by slippage of the pump, passive leaks or a subpopulation of incompletely sealed vesicles. Hara and Kasai (1977) accounted for the leak and still observed a low stoichiometry that they attributed to poorly estimated data. In one view, this could be taken as evidence for slippage of the pump, in which the pump possesses an inherently variable stoichiometry. The evidence presented in this paper, however, suggests that a

small population of incompletely sealed vesicles is responsible for contributing ATPase activity but no observable calcium fluxes. When the total ATPase activity is corrected for this uncoupled activity, the net ATPase of the competent vesicles is on the same order as the passive calcium efflux (Fig. 11). This implies that the calcium pump remains tightly coupled even under conditions of steady state uptake, or static head. Taken together, our data suggest that the Ca-ATPase activity of cardiac SR remains tightly coupled to calcium transport even at steady state uptake conditions. Under these conditions, the pump slows in order to balance a parallel passive leak of calcium. The coupling ratio appears to be close to 1.0.

This work was supported in part by a grant-in-aid from the American Heart Association, Virginia Affiliate, Inc., and grant HL19485 from the National Heart, Lung and Blood Institute.

Received for publication 15 March 1983 and in final form 24 January 1984.

REFERENCES

Berman, M. C. 1982. Energy coupling and uncoupling of active calcium transport by sarcoplasmic reticulum. *Biochim. Biophys. Acta.* 694:95–121.

Bock, R. M., N.-S. Ling, S. A. Morrell, and S. H. Lipton. 1956. Ultraviolet absorption spectra of adenosine 5'-triphosphate and related 5'-ribonucleotides. *Arch. Biochem. Biophys.* 62:253–264.

Chamberlain, B. K., D. O. Levitsky, and S. Fleischer. 1983. Isolation and characterization of canine cardiac sarcoplasmic reticulum with improved Ca^{2+} transport properties. *J. Biol. Chem.* 258:6602–6609.

Chevallier, J., J. P. Bonnet, M. Galante, J. P. Tenu, and T. Gulik-Krzywicki. 1977. Functional and structural heterogeneity of sarcoplasmic reticulum preparations. *Biol. Cell.* 30:103–110.

Ebashi, S., and F. Lipmann. 1962. Adenosine triphosphate-linked concentration of calcium ions in a particulate fraction of rabbit muscle. *J. Cell. Biol.* 14:389–400.

Feher, J. 1984. Unidirectional calcium and nucleotide fluxes in sarcoplasmic reticulum. I. Interpretation of flux ratios for different reaction schemes. *Biophys. J.* 45:000–000.

Feher, J. J., and F. N. Briggs. 1980. The effect of calcium oxalate crystallization kinetics on the kinetics of calcium uptake and calcium ATPase activity of sarcoplasmic reticulum vesicles. *Cell Calcium.* 1:105–118.

Feher, J. J., and F. N. Briggs. 1982. The effect of calcium load on the calcium permeability of sarcoplasmic reticulum. *J. Biol. Chem.* 257:10191–10199.

Feher, J. J., and F. N. Briggs. 1983. Determinants of calcium loading at steady-state in sarcoplasmic reticulum. *Biochim. Biophys. Acta.* 727:389–402.

Guimaraes-Motta, H., and L. DeMeis. 1980. Pathway for ATP synthesis by sarcoplasmic reticulum ATPase. *Arch. Biochem. Biophys.* 203:395–403.

Hara, K., and M. Kasai. 1977. The mechanism of increase in the ATPase activity of sarcoplasmic reticulum vesicles treated with n-alcohols. *J. Biochem.* 82:1005–1017.

Hopfer, U. 1981. Kinetic criteria for carrier-mediated transport mechanisms in membrane vesicles. *Fed. Proc.* 40:2480–2485.

Inesi, G., M. Kurzmack, D. Kosk-Kosicka, D. Lewis, H. Scofano, and H. Guimaraes-Motta. 1982. Equilibrium and kinetic studies of calcium transport and ATPase activity in sarcoplasmic reticulum. *Z. Naturforsch. Teil C Biochem. Biophys. Biol. Virol.* 37:685–691.

Jones, L. R., and H. R. Besch. 1979. Calcium handling by cardiac sarcoplasmic reticlum. *Tex. Rep. Biol. Med.* 39:19–35.

Jones, L. R., and S. E. Cala. 1981. Biochemical evidence for functional heterogeneity of cardiac sarcoplasmic reticulum vesicles. *J. Biol. Chem.* 256:11809–11818.

King, E. J. 1932. The colorimetric determination of phosphorus. *Biochem. J.* 26:292–297.

Kurebayashi, N., T. Kodama, and Y. Ogawa. 1980. P^1, P^5-di(adenosine-5') pentaphosphate (Ap_5A) as an inhibitor of adenylate kinase in studies of fragmented sarcoplasmic reticulum from bullfrog skeletal muscle. *J. Biochem.* 88:871–876.

Levitsky, D. O., M. K. Aliev, A. V. Kuzmin, T. S. Levchenko, V. N. Smirnov, and E. I. Chazov. 1976. Isolation of calcium pump system and purification of calcium ion dependent ATPase from heart muscle. *Biochim. Biophys. Acta.* 443:468–484.

Makinose, M. 1973. Possible functional states of the enzyme of the sarcoplasmic calcium pump. *FEBS Lett.* 37:140–143.

Martonosi, A., and R. Feretos. 1964. Sarcoplasmic reticulum. I. The uptake of Ca^{++} by sarcoplasmic reticulum fragments. *J. Biol. Chem.* 239:648–658.

Ogawa, Y., and N. Kurebayashi. 1982. ATP-ADP exchange reaction by fragmented sarcoplasmic reticulum from bullfrog skeletal muscle. *J. Muscle Res. Cell Motil.* 3:39–56.

Ronzani, N., A. Migala, and W. Hasselbach. 1979. Comparison between ATP-supported and GTP-supported phosphate turnover of the calcium-transporting sarcoplasmic reticulum membranes. *Eur. J. Biochem.* 101:593–606.

Suko, J., and W. Hasselbach. 1976. Characterization of cardiac sarcoplasmic reticulum ATP-ADP phosphate exchange and phosphorylation of the calcium transport adenosine triphosphatase. *Eur. J. Biochem.* 64:123–130.

Tada, M., M. A. Kirchenberger, D. I. Repke, and A. M. Katz. 1974. The stimulation of calcium transport in cardiac sarcoplasmic reticulum by adenosine 3':5'-monophosphate-dependent protein kinase. *J. Biol. Chem.* 249:6174–6180.

Tada, M., M. Yamada, F. Ohmori, T. Kuzuya, M. Inui, and H. Abe. 1980. Transient state kinetic studies of Ca-dependent ATPase and calcium transport by cardiac sarcoplasmic reticulum. *J. Biol. Chem.* 255:1985–1992.

Takakuwa, Y., and T. Kanazawa. 1982. Role of Mg in the Ca-Ca exchange mediated by the membrane-bound (Ca,Mg)-ATPase of sarcoplasmic reticulum vesicles. *J. Biol. Chem.* 257:10770–10775.

Takenaka, H., P. N. Adler, and A. M. Katz. 1982. Calcium fluxes across the membrane of sarcoplasmic reticulum vesicles. *J. Biol. Chem.* 257:12649–12656.

Verjovski-Almeida, S., M. Kurzmack, and G. Inesi. 1978. Partial reactions in the catalytic and transport cycle of sarcoplasmic reticulum ATPase. *Biochemistry.* 17:5006–5013.

Waas, W., and W. Hasselbach. 1981. Interference of nucleoside diphosphates and inorganic phosphate with nucleoside triphosphate-dependent calcium fluxes and calcium-dependent nucleoside-triphosphate hydrolysis in membranes of sarcoplasmic reticulum vesicles. *Eur. J. Biochem.* 116:601–608.

Warren, G. B., P. A. Toon, N. J. M. Birdsall, A. G. Lee, and J. C. Metcalfe. 1974. Reconstitution of a calcium pump using defined membrane components. *Proc. Natl. Acad. Sci. USA.* 71:622–626.